

RSC Advances



This is an *Accepted Manuscript*, which has been through the Royal Society of Chemistry peer review process and has been accepted for publication.

Accepted Manuscripts are published online shortly after acceptance, before technical editing, formatting and proof reading. Using this free service, authors can make their results available to the community, in citable form, before we publish the edited article. This *Accepted Manuscript* will be replaced by the edited, formatted and paginated article as soon as this is available.

You can find more information about *Accepted Manuscripts* in the [Information for Authors](#).

Please note that technical editing may introduce minor changes to the text and/or graphics, which may alter content. The journal's standard [Terms & Conditions](#) and the [Ethical guidelines](#) still apply. In no event shall the Royal Society of Chemistry be held responsible for any errors or omissions in this *Accepted Manuscript* or any consequences arising from the use of any information it contains.

1 **Cathepsin B-Sensitive Cholesteryl Hemisuccinate-Gemcitabine Prodrug Nanoparticles:**
2 **Enhanced Cellular Uptake and Intracellular Drug Controlled Release**

3
4 Yanyun Xu[§], Jianqi Geng⁺, Ping An[§], Yan Xu[§], Jin Huang^{§+}, Wei Lu[§], Jiahui Yu^{§1}

5 **Abstract**

6 Gemcitabine [2', 2'-difluoro-2'-deoxycytidine (dFdC)], firstline treatment for pancreatic
7 cancer in clinic, is a cytotoxic nucleoside analogue. Nucleoside transporters are required in the
8 transport of gemcitabine into cells since it is a hydrophilic compound. Actually, there are
9 significant drawbacks for the application of gemcitabine in clinic, including short half-life and
10 serious side effects. In order to overcome the mentioned drawbacks, a novel prodrug, cholesteryl
11 hemisuccinate-gemcitabine (CHSdFdC), was synthesized through covalently coupling the amino
12 group of gemcitabine with carboxylic group of cholesteryl hemisuccinate. The amphiphilic
13 prodrug self-assembled spontaneously as nanoparticles in aqueous media confirmed by
14 transmission electron microscope (TEM). Dynamic light scattering (DLS) measurement revealed
15 the mean particle size is approximately 200 nm in aqueous media. The CHSdFdC nanoparticles
16 displayed accumulative controlled drug release in simulated lysosome condition (pH 5.0 NaAc
17 buffer solution contained cathepsin B), the amount of drug release reached up to 80 % within 10 h.
18 However, there was almost no drug release in pH 7.4 PBS and pH 5.0 NaAc buffer solutions
19 without cathepsin B. All these results indicated the intracellular controlled drug release manner of
20 CHSdFdC nanoparticles. The controlled release of dFdC from CHSdFdC nanoparticles related
21 closely to cleavage of amide bond by cathepsin B. The CHSdFdC nanoparticles exhibited

¹ Corresponding author. Tel. /fax: +86 21 6223 7026. E-mail address: jhyu@sist.ecnu.edu.cn

(Jiahui Yu)

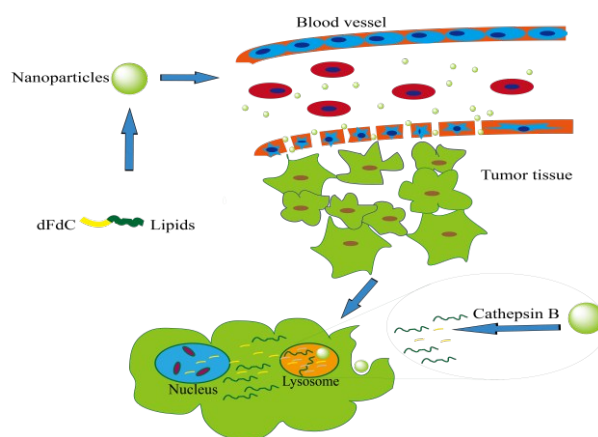
1 increased ability of inhibiting the cells growth compared with gemcitabine *in vitro*. Meanwhile,
2 CHSdFdC nanoparticles exhibited enhanced cellular uptake ability against Bxpc-3 cells, and the
3 amount of CHSdFdC was about 15 folds of gemcitabine during the 2.5 h incubation. All these
4 results showed the CHSdFdC nanoparticles prodrug has great potential in the treatment of
5 pancreatic cancer.

6

7 **1 Introduction**

8 Gemcitabine [2', 2'-difluoro-2'-deoxycytidine (dFdC)] has been proved to be a potent
9 cytotoxic nucleoside analogue demonstrated efficacy in the treatment of various solid tumors,
10 including colon, lung, pancreatic, breast, bladder and ovarian cancers ^[1-3]. In order to achieve
11 therapeutic effect, gemcitabine must be transported into cells. Membrane proteins called
12 nucleoside transporters are required in the transport of gemcitabine because it is a hydrophilic
13 compound. The main transporter types include hENT₁, hENT₂, hCNT₁ and hCNT₃ ^[4]. Nucleoside
14 transporter deficiency would make it difficult for gemcitabine to be transported into cells. In
15 addition, as a traditional chemotherapeutic drug, gemcitabine is difficult to accumulate at tumor
16 tissue selectively, which lead to undesired side effects and inadequate drug concentrations
17 reaching tumor, despite it is a primary drug for cancer treatment ^[5, 6, 7, 8]. In this paper, in order to
18 make it easier for gemcitabine to enter cells, especially nucleoside transporter deficiency cells, the
19 cholestery-hemisuccinate-gemcitabine conjugate was fabricated into nanoparticles to change the
20 approach that gemcitabine enter cells. As a result, gemcitabine would enter cells *via* endocytosis
21 rather than transport by nucleoside transporters. In addition, nanodrug delivery system could use
22 enhanced permeability and retention (EPR)(Fig.1) effect to promote the drugs targeting tumor
23 tissue selectively, leading to potentially enhanced antitumor effect and decreased side effects ^{[5,}

1⁹⁻¹⁴. Numerous nanodrug or nanaodrug candidates have been approved for clinical applications or
2 under clinical trials at different stages^[13, 15, 16]. After being transported into cells, a part of
3 gemcitabine is deaminized by cytidine deaminase into inactive uracil derivative (dFdU)
4 intracellularly, hence resulting in a short half-life^[17]. Acylation of N⁴-amino group of the
5 pyrimidine ring of dFdC would protect the amino group from being rapidly degraded by cytidine
6 deaminase. Taking the strategy of nanodrug delivery system, Couvreur's group covalently
7 coupled gemcitabine with squalenic acid, and the resultant 4-(N)-tris-nor-squalenoyl-gemcitabine
8 (SQdFdC) prodrug self-assembled into nanoparticles, which were shown to overcome
9 gemcitabine resistance in murine leukemia cells (i.e., L1210 10K)^[18], human leukemia cells (i.e.,
10 CEM/ARAC8C)^[18], and human pancreatic cancer cells (i.e., Panc-1)^[19]. It was concluded that
11 SQdFdC nanoparticles enabled the partial circumvention of three well-known resistance
12 mechanisms to gemcitabine, including the deficiency of nucleoside transporters, insufficient
13 activity of deoxycytidine kinase (dCK), and inactivation by deaminases^[20]. Zhengrong Cui *et al.*
14 have reported that 4-(N)-stearoyl gemcitabine (GemC18), a stearic acid amide derivative of
15 gemcitabine, could effectively inhibit the growth of gemcitabine resistance TC-1-GR tumors in
16 mice, and in contrast, the molar equivalent dose of gemcitabine hydrochloride did not show any
17 activity against the growth of the TC-1-GR tumors^[21].



18
19 Fig.1 Illustration of EPR effect and intracellular controlled release of dFdC from CHSdFdC

1 Cholesterol is an indispensable substance in the formation of cell membranes. As the basic
2 component of membrane, cholesterol accounts for over 20 % of plasma membrane lipids.
3 Meanwhile, cholesterol is one of the important components of the liposome membranes. It has
4 been found that cholesterol can maintain the fluidity of membrane ^[22]. As a component of the
5 biofilm, cholesterol exist excellent biocompatibility ^[23]. Because of all these properties,
6 cholesterol is important to membrane fusion, which is an essential procedure for endocytosis ^[24].
7 ^{25]}.Then, it is expected that the anti-tumor drug modified with cholesterol will display enhanced
8 ability of cellular uptake to increase their therapeutic effect and decrease the side effects.

9 In this study, cholesteryl hemisuccinate was used to modify gemcitabine to give CHSdFdC
10 prodrug. The prodrug could self-assemble into nanoparticles in aqueous media. The properties of
11 the nanoparticles were investigated, such as critical micelle concentration (CMC), mean particle
12 size and size distribution, zeta potential, morphology and colloidal stability. The process of drug
13 release from the nanoparticles and cellular uptake by Bxpc-3 cells *in vitro* were investigated in
14 detail. Meanwhile, we assayed the ability of inhibiting the growth of Bxpc-3 cells of the prodrug
15 *in vitro*. The nanoparticles have the capability to realize intracellular controlled release of
16 gemcitabine and reduce side effects because amide bond of the prodrug nanoparticles can be
17 degraded by cathepsin B, an enzyme exists in lysosome.

18

19 **2 Experimental**

20 **2.1 Materials and cells**

21 Cholesterol was purchased from J&K Chemical Ltd.. Gemcitabine hydrochloride was
22 purchased from Shang Hai PuYi Chemical Co., Ltd.. Gemcitabine base was purchased from
23 Shanghai Demo Medical Tech Co., Ltd.. EDCI and DMAP was purchased from Energy Chemical..

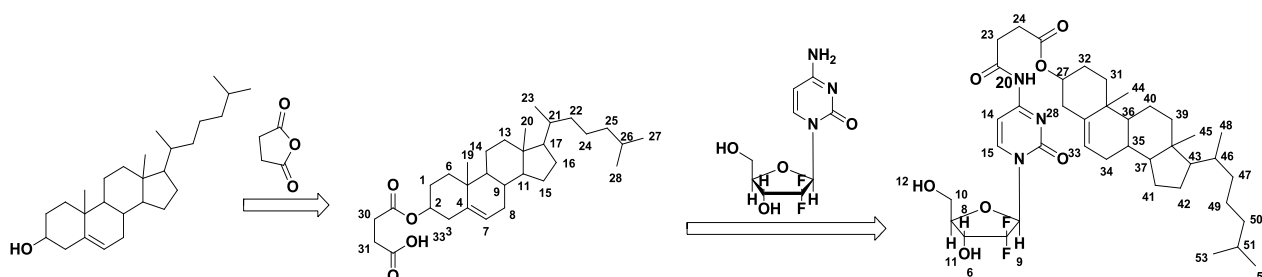
1 Other chemicals were purchased from Sinopharm Chemical Reagent Co., Ltd.. DCM, DMF and
 2 THF were dried and redistilled before use.

3 The Bxpc-3 cell line is a kind of human pancreatic cancer cell line, which was purchased
 4 from the Institute of Biochemistry & cell Biology, Chinese Academy of Science.

5 2.2 Characterization of compounds

6 ^1H NMR spectra were recorded with a Bruker Avarice TM 400 NMR spectrometer. The
 7 Fourier transform infrared spectra (FT-IR) were obtained with a Nicolet Nexus 670 spectrometer.
 8 The samples were pressed into pellets with KBr.

9 2.3 Synthesis of cholesteryl hemisuccinate-gemcitabine (CHSdFdC)



11 Scheme.1 Synthesis scheme of cholesteryl hemisuccinate-gemcitabine (CHSdFdC)

12 Succinic anhydride (1.2 mmol) was added to stirred solution of cholesterol (1.0 mmol) in
 13 toluene. The mixture was refluxed for 3 h, cooled to room temperature and filtered. The
 14 precipitate was collected and recrystallized with ethanol for twice, the cholesteryl hemisuccinate
 15 was obtained (yield: 82.8 %). IR (neat, cm^{-1}) 3442 (-OH), 2943-2860 (-CH₂-), 1712 (-C=O), 1176
 16 (C-O-C). ^1H NMR (400 MHz, CDCl_3) δ : 0.68 (3 H, s, 20-H), 0.8~2.4 (28 H, 1-H₂, 3-H₂, 6-H₂,
 17 8-H₂, 9-H₁, 10-H₁, 11-H₁, 13-H₂, 14-H₂, 15-H₂, 16-H₂, 17-H₁, 21-H₁, 22-H₂, 24-H₂, 25-H₂, 26-H₁),
 18 0.87 (6H, d, J=6.4Hz, 27-H₃, 28-H₃), 0.92 (3H, d, J=6Hz, 23-H₃), 1.02 (3H, s, 19-H₃), 2.61
 19 (2H, m, COCH₂), 2.68 (2H, m, CH₂CO), 4.64 (1H, m, 2-H₁), 5.37 (1H, m, 7-H₁)

20 Triethylamine (1.4 mmol) was added to stirred solution of cholesteryl hemisuccinate (1.2

1 mmol) in anhydrous THF (3 mL), under nitrogen. The mixture was cooled to -15 °C, and the
2 solution of isobutyl chloroformate (1.2 mmol) in anhydrous THF (3 mL) was added dropwise.
3 The mixture was stirred at -15 °C for 15 min and the solution of gemcitabine hydrochloride (1.2
4 mmol) and triethylamine (1.4 mmol) in anhydrous DMF (5 mL) was added dropwise to the
5 mixture at the same temperature, then the mixture was stirred for another 0.5 h at -15 °C. After
6 being stirred for 72 h at room temperature, the reaction mixture was concentrated. Aqueous
7 sodium hydrogen carbonate was added and the mixture was extracted with DCM (3×50 mL). The
8 combined extracts were washed with water, dried over MgSO₄, and concentrated. The crude
9 product was purified by chromatography on silica gel eluting with 1 % to 5 % methanol in
10 dichloromethane to give cholesteryl hemisuccinate-gemcitabine as amorphous white solid
11 (yield:32%). IR (neat, cm⁻¹) 3500 (-CO-NH-), 3000 (-C=C-), 1665 (-CO-NH-), 1400 (-CO-NH-),
12 1065 (C-O). ¹H NMR (400M, DMSO-d₆) δ: 0.65 (3H, s, 45-H₃), 0.85 (6H, dd, 52-H₃, 53-H₃),
13 0.90 (3H, d, 48-H₃), 0.96 (3H, s, 44-H₃), 0.8-2.4 (28H, 28-H₂, 31-H₂, 32-H₂, 34-H₂, 35-H₁, 36-H₁,
14 37-H₁, 39-H₂, 40-H₂, 41-H₂, 42-H₂, 43-H₁, 46-H₁, 47-H₂, 49-H₂, 50-H₂, 51-H₁), 2.56(2H, m,
15 COCH₂), 2.69 (2H, m, CH₂CO), 3.66 (1H, m, 6-H₁), 3.80 (1H, d, 10-H₁), 3.89 (1H, d, 10-H₁),
16 4.19 (1H, m, 11-H₁), 4.45 (1H, m, 27-H₁), 5.28 (1H, t, 33-H₁), 5.34 (1H, d, 8-H₁), 6.18 (1H, t,
17 12-H₁), 6.31 (1H, d, 9-H₁), 7.24 (1H, d, 15-H₁), 8.24 (1H, d, 14-H₁), 11.08 (1H, s, 20-H₁).

18 2.4 Nanoparticle fabrication and the critical micelle concentration

19 The CHSdFdC (5 mg) was dissolved in 10 mL THF, and the solution was added dropwise
20 into 10 mL ultrapure MilliQ® water with constant stirring at 500 rpm. After stirring, the solution
21 was loaded into a dialysis tube (MWCO 1000) and dialyzed against 12 L (4 L×3) deionized water
22 for 24 h.

23 The critical micelle concentration (CMC) was determined using pyrene as a fluorescence

1 probe ^[26]. The concentration of CHSdFdC varied from 2×10^{-4} to 0.1 mg/mL with a fixed pyrene
2 concentration of 6×10^{-7} mol/L. The fluorescence spectra were measured on an F-4500
3 fluorescence spectrophotometer (Hitachi F-4500) with an excitation wavelength of 335 nm. The
4 I_{373} / I_{384} ratio of the fluorescence intensity in the emission spectra of pyrene was analyzed for the
5 calculation of the CMC. The experiment was performed in triplicate. The mean and corresponding
6 standard deviations (mean \pm SD) are shown in the results.

7 **2.5 Formulation and characterization of CHSdFdC nanoparticles**

8 CHSdFdC nanoparticles were prepared by nanoprecipitation. Briefly, CHSdFdC (5 mg) was
9 dissolved in THF (5 mL) and the solution was added dropwise into 10 mL ultrapure MilliQ®
10 water under constant stirring at 500 rpm. The form of CHSdFdC nanoparticles occurred
11 spontaneously. THF was completely evaporated using a rotary evaporator at 37 °C to obtain an
12 aqueous suspension of pure CHSdFdC nanoparticles. The nanoparticles suspension has been
13 analyzed using RP-HPLC to verify the actual concentration of CHSdFdC in the final product.

14 The mean particle size, size distribution, polydispersity index (PDI) and zeta potential were
15 determined using dynamic light scattering (DLS) (ZetasizerNano ZS, Malvern Instruments, UK).
16 The measurements were made after dilution of the nanoparticles suspension with ultrapure
17 MilliQ® water.

18 The morphology of the nanoparticles was observed by transmission electron microscopy
19 (TEM) (JM-2100, Japanese). A drop of aqueous nanoparticles suspension was deposited onto a
20 300 mesh copper grid coated with a thin carbon film. The grids were dried at room temperature
21 and observed by TEM.

22 **2.6 Colloidal stability of nanoparticles**

23 The colloidal stability of nanoparticles was investigated by measuring variation of mean

1 particle size of the nanoparticles. The nanoparticles were diluted with PBS to maintain the final
2 concentration of CHSdFdC was 2mg/mL and stored at 4 °C for 28 days. Meanwhile, the
3 nanoparticles were diluted with cell culture medium (RPMI 1640 (Gibco BRL, Paris, France)) to
4 maintain the final concentration of CHSdFdC was 2mg/mL and incubated at 37 °C for 10 days.
5 The experiment was performed in triplet. The mean and corresponding standard deviations (mean
6 \pm SD) are shown in the results.

7 **2.7 Cell line and culture**

8 Human pancreatic cancer cell line Bxpc-3 was purchased from the Institute of Biochemistry
9 & cell Biology, Chinese Academy of Science. Bxpc-3 cells were cultured in RPMI 1640 (Gibco
10 BRL, Paris, France) supplemented with 10 % fetal bovine serum (FBS, HvClone, Logan UT) and
11 1 % penicillin and streptomycin. The cell line was incubated at 37 °C in humidified 5 % CO₂
12 atmosphere. When a cell confluence of 90 % was reached, they were routinely trypsinized and
13 subcultured.

14 **2.8 Drug release from the CHSdFdC nanoparticles**

15 Release of gemcitabine from the CHSdFdC nanoparticles in an aqueous buffer solution at
16 different pH values (pH 5.0, pH 7.4) was measured by RP-HPLC with an Agilent 1200 (Agilent
17 Technologies INC., Shanghai Branch) using a Zorbax Eclipse XDB-C18 column (5 μ m, 4.6 mm \times
18 250 mm) at 30 °C. The CHSdFdC (1 mg/mL in DMSO), 60 μ L, was dispersed in 2 mL of three
19 different media including PBS (pH 7.4), sodium acetate buffer solution (pH 5.0), sodium acetate
20 buffer solution (pH 5.0) contained 60 μ L cathepsin B (U-activity unit=10 U/mL). The samples
21 were kept in a THZ-C isothermal shaker at 37 °C and 150 rpm. At the predetermined time point,
22 100 μ L of the sample solution was withdrawn, and same amount of acetonitrile was added
23 immediately. The accumulative drug release was measured by RP-HPLC using methanol as the

1 mobile phase. The flow rate of the mobile phase was 1 mL/min. The Agilent 1200 Uv/vis detector
2 was set at 254 nm. The release percentage of dFdC was calculated from the ratio of peaks area
3 assigned to free dFdC and CHSdFdC. The experiment was performed in triplet. The mean and
4 corresponding standard deviations (mean \pm SD) are shown in the results. The cathepsin B is a
5 kind of lysosomal enzyme which does not exist in human blood ^[27, 28]. It is reported that the pH
6 value of lysosome is about 5.0 ^[29]. What we expect is that the prodrug is stable when it circulates
7 in human blood whereas it can be degraded with presence of cathepsin B to release controlled
8 release of dFdC from CHSdFdC prodrug. In the paper, the PBS with pH 7.4 was used to simulate
9 the pH value of human blood, pH 5.0 buffer solution with cathepsin B was used to simulate the
10 condition of lysosome, pH 5.0 buffer solution without cathepsin B was used to clarify that
11 cathepsin B is an indispensable trigger in the controlled drug release.

12 **2.9 *In vitro* ability of inhibiting the growth of Bxpc-3 cells assay**

13 The ability of inhibiting the growth of tumor cells of CHSdFdC nanoparticles was
14 investigated and compared with dFdC as positive control by MTT [3-(4, 5-dimethylthiazol-2-yl)-2,
15 5-diphenyl tetrazolium bromide] assay against Bxpc-3 cell line. Briefly, 4000 cells per well were
16 incubated in 100 μ L of complete culture medium (RPMI 1640 (Gibco BRL. Paris, France)
17 supplemented with 10 % fetal bovine serum (FBS, HvClone , Logan UT) and 1 % penicillin and
18 streptomycin) in 96-well plates for 24 h. The cells were then exposed to a series of concentrations
19 of CHSdFdC nanoparticles, free dFdC or free CHS in 100 μ L fresh complete culture medium for
20 72 h. The drug concentration in the case of CHSdFdC nanoparticles is equivalent to dFdC
21 concentration. At the end of the incubation period, 20 μ L of MTT solution (5 mg/mL) in PBS was
22 added to each well. The culture medium was gently replaced by 100 μ L of dimethylsulfoxide in
23 order to dissolve the formazan crystals after 4 h incubation. The optical density (OD) was

1 measured at 570 nm with an automatic BIO-TEK microplate reader (Powerwave XS, USA), and
2 the cell viability was calculated through the following equation:

$$3 \quad \text{Cell viability (\%)} = (\text{OD}_{\text{sample}}/\text{OD}_{\text{control}}) \times 100 \%. \quad (1)$$

4 The $\text{OD}_{\text{sample}}$ represents an OD value from a well that treated with samples, and $\text{OD}_{\text{control}}$ comes
5 from a well that treated with cell culture medium only. Each experiment was performed in
6 sextuplet. The mean and corresponding standard deviations (mean \pm SD) are shown in the results.

7 **2.10 Cellular uptake**

8 The cellular uptake of CHSdFdc nanoparticles was quantitatively measured by RP-HPLC.
9 The Bxpc-3 cells were seeded in 6-wells plate at a density of 2.5×10^5 cells/well in 2 mL of
10 culture medium and incubated for 24 h. The original cell culture medium was replaced with 2
11 mL fresh culture medium contained dFdc and CHSdFdc (dFdc: 0.1 mg/mL). The cells were
12 cultured for another 0.5 h, 1.5 h and 2.5 h, respectively. At the predetermined time point, the cell
13 culture medium was discarded, and 2 mL of 1 % SDS was added to make cell membrane lytic
14 after the wells were washed with cold PBS for three times carefully. The cell lysate was
15 dissolved in 200 μ L mixture of methanol and acetonitrile (v: v=1:1) after freeze drying. The
16 concentrations of dFdc and CHSdFdc were measured by RP-HPLC. Experiments were carried
17 in triplicates. Means and corresponding standard deviations (mean \pm SD) were shown as results.

18 **2.11 Statistical data analysis**

19 Statistical data analysis was performed using Student's t-test.

20

21 **3 Results and discussion**

22 **3.1 Synthesis of cholesteryl hemisuccinate-gemcitabine (CHSdFdc)**

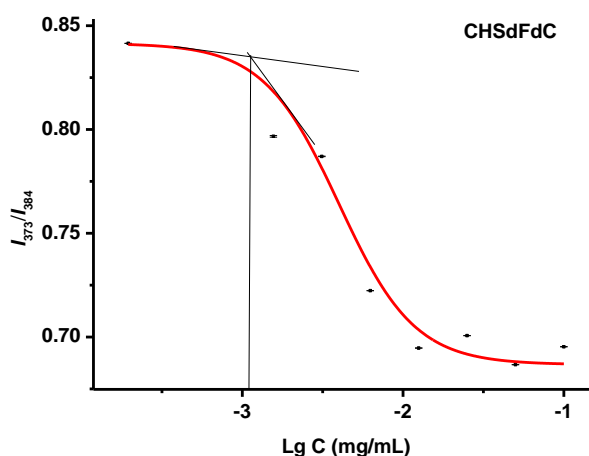
23 Cholesteryl hemisuccinate was synthesized through esterification reaction between

1 cholesterol and succinic anhydride. During the reaction, DMAP was used as catalysis. The
2 synthesis scheme of cholesteryl hemisuccinate is shown in Scheme.1. The structure of the product
3 was confirmed by NMR, and the detailed data of the chemical shifts are displayed in part 2.3. The
4 structure was confirmed from the appearance of the peaks at 2.61 and 2.68 ppm which belong to
5 succinic anhydride, 0.68, 0.87, 0.92, 1.02, 4.64, 5.37 ppm which belong to cholesterol. The ratio
6 of succinic acid to cholesterol was equal to 1:1, which was confirmed by calculation of the
7 integral ratios of the protons at 5.37 ppm (multiplet) assigned to 7-H signal of cholesterol and
8 2.61 ppm (multiplet) assigned to the methylene protons signal of succinic acid. In order to further
9 confirm the structure of the product, Fourier transform infrared spectra were recorded. The FT-IR
10 spectra data showed a new absorption appearance located at 1712 cm^{-1} assigned to carboxyl group
11 and 3442 cm^{-1} assigned to hydroxyl group.

12 The CHSdFdC was synthesized through covalently coupling the amino group of gemcitabine
13 on pyridine ring and the carboxyl group of cholesteryl hemisuccinate. The synthesis scheme is
14 shown in Fig.2. The structure was confirmed by NMR, and the detailed data of the shifts are
15 displayed in part 2.3. The structure was confirmed from the appearance of the peaks at 11.08 ppm,
16 which belong to amide bond and the disappearance of the peaks at 7.41 ppm which belong to the
17 amino group of gemcitabine. The integral ratios of the protons at 11.08 ppm (single) assigned to
18 amide proton signal and 0.65 ppm (single) assigned to the methyl protons signal of cholesteryl
19 hemisuccinate were 1:3, indicating that the ratio of gemcitabine and cholesteryl hemisuccinate in
20 the CHSdFdC was equal to 1:1. In order to further confirm the structure of CHSdFdC, Fourier
21 transform infrared spectra were recorded. The FT-IR spectra data showed a new absorption
22 appearance located at 3500 cm^{-1} assigned to the amide bond.

23 3.2 CMC measurement of CHSdFdC

1 The CHSdFdC formed nanoparticles in aqueous media due to its amphiphilic structure. CMC
2 was measured by fluorospectrophotometer with pyrene as a probe. The plot of the intensity ratio
3 I_{373}/I_{384} of the pyrene emission spectra against the logarithm of the CHSdFdC concentration is
4 shown in Fig.3. The CMC value can be determined at the CHSdFdC concentration of onset of the
5 I_{373}/I_{384} ratio decrease. When the concentration of CHSdFdC reaches the CMC, there is a sudden
6 change of I_{373}/I_{384} in the fluorescence spectra due to the transfer of pyrene from a polar
7 environment to a non-polar environment caused by the formation of nanoparticles. The CMC of
8 CHSdFdC is 0.001 mg/mL, as shown in Fig.2. The CMC of CHSdFdC was very low, indicating it
9 is rather stable against dilution.



10

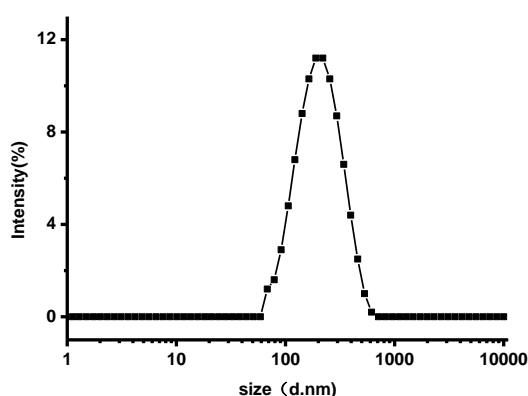
11 Fig.2 Intensity ratio I_{373}/I_{384} of the pyrene emission fluorescence spectra as a function of the
12 logarithm concentration of the CHSdFdC (means \pm SD, n=3)

13 3.3 Characterization of the nanoparticles

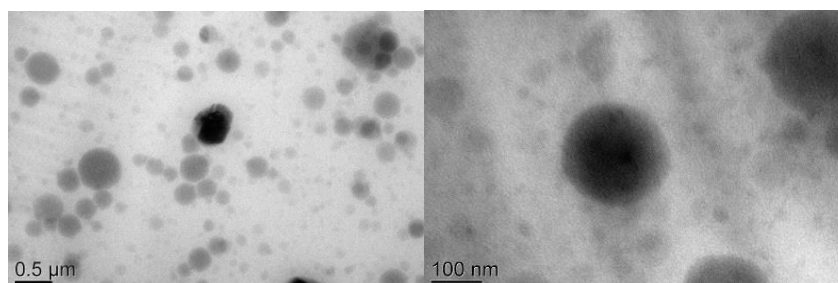
14 Particle size is an important factor that affects their *in vivo* performance and
15 pharmacokinetics for nanoparticles. Tumors, unlike most healthy tissues, possess a leaky
16 vasculature that allows the passage of colloidal particles with size in the range of 50-200 nm^[30-32].
17 In this research, the mean particle size and size distribution, zeta potential were measured by DLS
18 in aqueous media at room temperature. The mean particle size was 200 nm, as shown in Fig.3A.

1 The main hydrodynamic diameter of the CHSdFdC nanoparticles was between 40 and 500 nm.
2 This demonstrated that the nanoparticles were able to pass through the large pores of the tumor
3 blood vessel to target the tumor tissue. The nanoparticles showed negative potential at around
4 -0.06 mV in the measurement of zeta potential, suggesting potential capacity for prolonging the
5 circulation time in blood because nanoparticles with positive surface charges are inclined to
6 agglomerate due to interaction with serum protein in human blood ^[33].

7 The morphology of the nanoparticles was observed by transmission electron microscopy
8 (TEM), as shown in Fig.3B and Fig.3C. The mean particle size was approximately 200 nm in a
9 dehydrated state. The size measured by TEM was very close to that measured by DLS in aqueous
10 media.



A



B

C

15 Fig.3 (A) Size and size distribution of CHSdFdC nanoparticles (B, C) Transmission
16 election microscopy (TEM) of CHSdFdC nanoparticles

3.4 Colloidal stability of CHSdFdC nanoparticles

The colloidal stability of the nanoparticles was investigated by measuring the variation of mean particle size. The nanoparticles were diluted with PBS and stored at 4 °C for 28 days. This is the storage condition for CHSdFdC nanoparticles suspension. Meanwhile, the nanoparticles were diluted with cell culture medium (RPMI 1640 (Gibco BRL, Paris, France)) and incubated at 37 °C for 10 days. This condition was used to simulate the human plasma, in order to assay the stability of CHSdFdC nanoparticles when it circulates in human plasma. It demonstrated that the CHSdFdC nanoparticles are stable at 4 °C in PBS as well as at 37 °C in cell culture medium (RPMI 1640 (Gibco BRL, Paris, France)), with no significant variation of the mean particle size was observed, as shown in Fig.4A and Fig.4B.

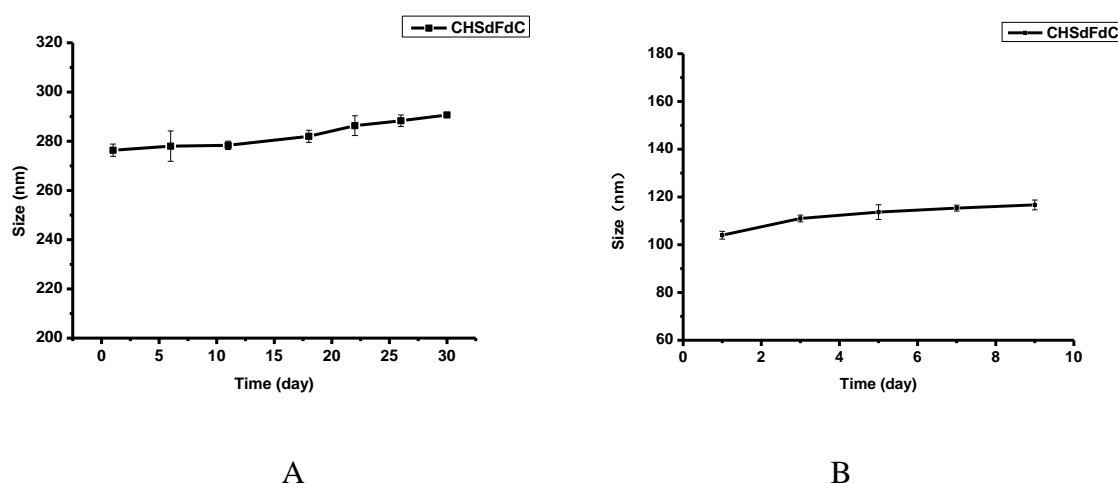
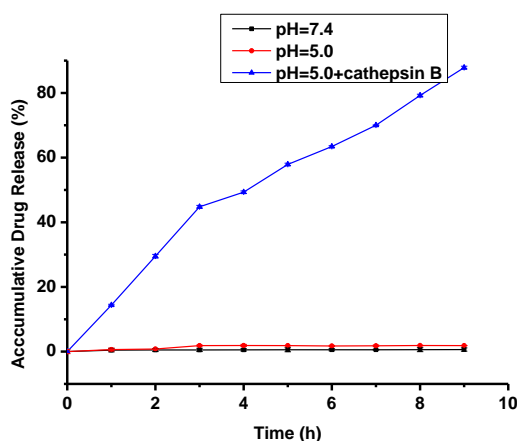


Fig.4 (A) Variation of the mean particle size of CHSdFdC nanoparticles at 4 °C in PBS (means \pm SD, n=3) (B) Variation of the mean particle size of CHSdFdC nanoparticles at 37 °C in cell culture medium (means \pm SD, n=3)

3.5 Drug release from the CHSdFdC nanoparticles

The amide bond could be degraded by cathepsin B which exists in lysosome. Thus, there is possibility for dFdC to release from the CHSdFdC nanoparticles at the presence of cathepsin B.

1 As shown in Fig.5, the release of dFdC was very slow under weakly acid condition (pH 5.0 NaAc
 2 buffer solution) or neutral pH condition (pH 7.4 PBS), the amounts were 0.64 % and 1.84 %
 3 within 10 h, respectively. On the other hand, the release of dFdC was much faster under the
 4 weakly acid condition (pH 5.0 NaAc buffer solution) in the presence of cathepsin B, the
 5 accumulative amount of drug release reached up to 80 % within 10 h. These results demonstrated
 6 the CHSdFdC nanoparticles had great potential to realize intracellular release of dFdC.



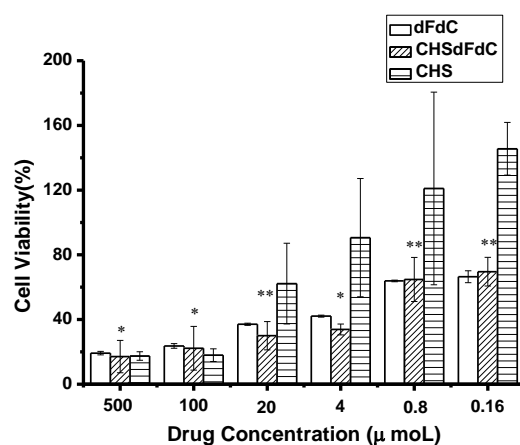
7
 8 Fig.5 Accumulative drug release of dFdC from CHSdFdC nanoparticles at 37 °C

9 (means \pm SD, n=3)

10 3.6 *In vitro* ability of inhibiting growth of Bxpc-3 cells assay

11 The *in vitro* ability of inhibiting growth of tumor cells of the CHSdFdC nanoparticles was
 12 evaluated with a human pancreatic cancer cell line Bxpc-3 *via* MTT assay. Representative
 13 concentration-growth inhibition curves showed the effects of treatment with free dFdC and
 14 CHSdFdC nanoparticles on the growth of Bxpc-3 cells after 72 h. As shown in Fig.7, both free
 15 dFdC and CHSdFdC nanoparticles inhibited cell growth in a dose-dependent manner, whereas the
 16 latter was more toxic than the former at the same concentration. It was thought that the increased
 17 cytotoxicity of the CHSdFdC resulted from two reasons .On one hand, CHSdFdC nanoparticles
 18 possess enhanced ability of cellular uptake, which make it easier to enter tumor cells. This was
 19 confirmed by the cellular uptake experiment. On the other hand, the released CHS, due to the

1 degradation of CHSdFdc nanoparticles prodrug by cathepsin B, also demonstrated ability of
 2 inhibiting the growth of Bxpc-3 cells, especially at high concentration as shown in Fig.6. It has
 3 been reported that CHS could incorporate into cell membrane to inhibit cell proliferation [34]. Only
 4 when the concentration of CHS reaches a certain high level, the cytotoxicity could be observed.
 5 And the result in this paper is consistent with the reported result [34].

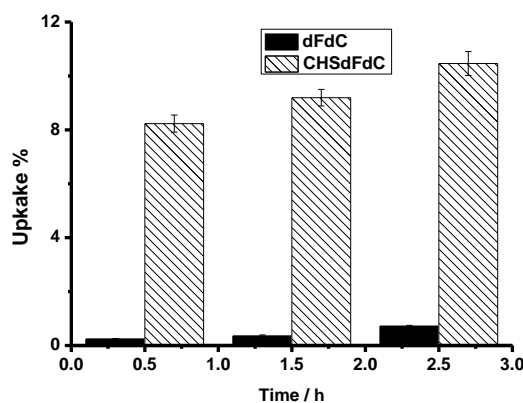


7
 8 Fig.6 Cell viability of free dFdc, CHSdFdc nanoparticle and CHS (means \pm SD, n=6, *
 9 P<0.01, ** P<0.05)

10 3.7 Cellular uptake

11 In order to confirm the hypothesis that the ability of cellular uptake of CHSdFdc
 12 nanoparticles is enhanced than dFdc, the amount of cellular uptake of CHSdFdc nanoparticles
 13 was measured by RP-HPLC, in the measurement, dFdc was used as control. As shown in Fig.7,
 14 the cellular uptake amount of CHSdFdc nanoparticles varied apparently while that of dFdc
 15 varied little, which is 15 folds of dFdc at the same culture period of 2.5 h. The conclusion was
 16 drawn that CHSdFdc nanoparticles could penetrate the cells much more easily than free dFdc,
 17 which improved the efficacy of inhibiting growth of tumor cells. The result in this paper showed
 18 that the CHSdFdc nanoparticles could be internalized much more easily than free dFdc, this
 19 result is related to the different uptake mechanism of dFdc and CHSdFdc nanoparticles. But the

1 cytotoxic activity of the drug and the prodrug are similar, this result is due to the incomplete
2 cleavage of CHSdFdC to release dFdC which actually demonstrate the effect of inhibiting cells
3 growth.



4
5 Fig.7 Cellular uptake of dFdC and CHSdFdC (means \pm SD, n=3)

6 Conclusions

7 The amphiphilic prodrug, CHSdFdC, which can self-assemble in aqueous media
8 spontaneously to form nanoparticles, was synthesized. The mean particle size of the nanoparticles
9 is about 200 nm and the zeta potential is -0.06 mV. The nanoparticles are relatively stable at
10 storage condition and stimulate human plasma. Compared with free gemcitabine, the
11 nanoparticles exhibited increased ability of cellular uptake and inhibiting the growth of Bxpc-3
12 cells *in vitro*. Moreover, the CHSdFdC nanoparticles prodrug displayed intracellular controlled
13 drug release of gemcitabine from the nanoparticles. The nanoparticles provide a new approach to
14 deliver gemcitabine to cancer cells. Generally speaking, the CHSdFdC has a great potential as
15 prodrug for pancreatic cancer and other tumor therapy.

16 Acknowledgements

17 The research work was supported by the International Science & Technology Cooperation
18 Program of China, Ministry of Science and Technology of China (2013DFG32340), Shanghai
19 Municipality Commission for Special Project of Nanometer Science and Technology

1 (11nm0506000), and the EU-FP 7 project (MARINA 263215).

2

3 **Notes and references**

4 § Institute of Drug Discovery and Development, Shanghai Engineering Research Center of
5 Molecular Therapeutics and New Drug Development, East China Normal University, Shanghai
6 200062, PR China

7 † College of Chemical Engineering, Wuhan University of Technology, Wuhan 430070, PR
8 China

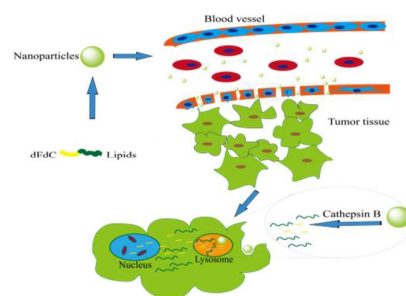
9 Corresponding authors. E-mail: jhyu@sist.ecnu.edu.cn (Prof. Jiahui Yu); Tel. /fax: +86 21 6223
10 7026

1 **References**

- 2 [1]Lund, B., Hansen, O. P., Theilade, K., Hansen, M., Neijt, J. P., *J. natl. Cancer Inst.*, 1994, **86**,
3 1530-1533.
- 4 [2] Anderson, H., Lund, B., bach, F., Thatcher, N., Walling, J., Hansen, H. H., *J. Clin. Oncol.*,
5 1994, **12**, 1821-1826.
- 6 [3] Catimel, G., Vermorken, J. B., Clavel, M., et al., *Ann. Oncol.*, 1994, **5**, 543-547.
- 7 [4] J.R. Mackey, R. S. Mani, M. Selner, D. Mowles, J. D. Young, J. S. Bett, C.R. Crawford, C. E.
8 Cass, *Cancer Res.* 1998, **58**, 4349-4357.
- 9 [5] D.Peer, J. M. Karp, S. Hong, O. C. Farokhzad, R. Margalit, R. Langer, *Nat Nanotechnol.* ,
10 2007, **2**, 751-760.
- 11 [6] F. M. Kievit, M. Zhang, *Adv. Mater.* 2011, **23**, 217-247.
- 12 [7]M. Ding, J. Li, X. He, N. Song, H. Tan, Y. Zhang, L. Zhou, Q. Gu, H. Deng, Q. Fu, *Adv. Mater.*,
13 2012, **24**, 3639-3645.
- 14 [8] M. T. Basel, T. B. Shrestha, D. L. Troyer, S. H. Bossmann, *ACS Nano.*, 2011, **5**, 2162-2175.
- 15 [9] T.M.Allen, P.R.Cullis, *Science.*, 2004, **303**, 1818-1822.
- 16 [10] M. Ferrari, *Nat. Rev. Cancer.*, 2005, **5**, 161-171.
- 17 [11] M. E. Davis, Z. Chen, D. M. Shin, *Nat. Rev. Drug Discovery*, 2008, **7**, 771-782.
- 18 [12] E. K. Chow, X. Q. Zhang, M. Chen, R. Lam, E. Robinson, H. Huang, D. Schaffer, E. Osawa,
19 A. Goga, D. Ho, *Sci. Transl. Med.*, 2011, **3**, 73-93.
- 20 [13] J. A. Barreto, W. O. Malley, M. Kubeil, B. Graham, H. Stephan, L. Spiccia, *Adv. Mater.*,
21 2011, **23**, 18-40.
- 22 [14] A. Schroeder, D. A. Hever, M. M. Winslow, J.E. Dahlman, G. W. Pratt, R. Langer, T. Jacks, D.
23 G., Anderson, *Nat. Rev. Cancer*, 2012, **12**, 39-50.

- 1 [15] R.K. Jain, T. Stylianopoulos, *Nat. Rev. Clin. Oncol.*, 2010, **7**, 653-664.
- 2 [16] W. J. Gradishar, S. Tjulandin, N. Davidson, H. Shaw, N. Desai, P. Bhar, M. Hawkins, J. O'
3 Shaughnessy, *J. Clin. Oncol.*, 2005, **23**, 7794-7803
- 4 [17] T. Neff, C. A. Blau, *Exp. Hematol.*, 1996, **24**, 1340-1346
- 5 [18] Reddy L H, Dubernet C, Mouelhi S L, Marque P E, Desmaele D, Couvreur P, *J. controlled*
6 *Release*, 2007, **124**, 20-27.
- 7 [19] Rejiba S, Reddy L H, Bigand C, Parmentier C, Couvreur P, hajri A, *Nanomedicine* , 2011, **7**,
8 841-849.
- 9 [20] Allain V, Bourgaux C, Couvreur P, *Nucleic Acid Res.*, 2012, **40**, 1891-1903.
- 10 [21] Woon-Gye Chung, Michael A. Sandoval, Brian R. Sloat, DharmikaS.P.Lansakara P,
11 Zhengrong Cui, *J. Controlled. Release*, 2012, **157**, 132-140.
- 12 [22] Ira Tabas, *J. Clin. Invest.*, 2002, **110**, 905-911.
- 13 [23] X.Tan et al., *Anal. Biochem.*, 2005, **337**, 111-120.
- 14 [24] Z. Chen, R.P. Rand, *Elasticity Biophysical Journal*, 1997, **73**, 267-276.
- 15 [25] Margaret C, Kielian, Ari Helenius, *J. Virol.*, 1984, **52**, 281-283
- 16 [26] R. Duncan, L. W. Seymour, K. B. O'Hare, et al., *J. Controlled Release*, 1992, **19**, 331-346.
- 17 [27] J.S. Mort, D.J. Buttle, *Int. J. Biochem. Cell Biol.*, 1997, **29**,715-720
- 18 [28] O. Vasiljeva, B. Turk, *Biochimie*, 2008, **90**, 380-386
- 19 [29] Shoji Ohkuma, Brian Poole, *Proc. Natl. Acad. Sci. USA*, 1978, **75**, 3327-3331
- 20 [30] F. Yuan, M. Leunig, S. K. Huang, D. A. Berk, *Cancer Rev.*, 1994, **54**, 3352-3356.
- 21 [31] R. K. Jain, *Adv. Drug Deliv. Rev.*, 1997, **26**, 71-90.
- 22 [32] N. Z. Wu, D. Da, T. L. Rudoll, D. Needham, et al., *Cancer Res.*, 1993, **53**, 3765-3770.
- 23 [33] X. Zhang, F. Du, J. Huang, *Colloids Surf. B* 2012, **100**, 155-162

- 1 [34] Z. Djuric, L.K. Heilbrun, S. Lababidi, C.K. Everett-Bauer, M.W. Fariss, *Cancer Lett.* 1997,
- 2 **111**, 133-139



Cholesteryl hemisuccinate-gemcitabine prodrug: enhanced cellular uptake and intracellular drug controlled release